20 ELEMENTS OF THE SANTA SUSANA FIELD LABORATORY SITE CONCEPTUAL MODEL OF CONTAMINANT TRANSPORT

SITE CONCEPTUAL MODEL ELEMENT DOCUMENT 4-1

Technical Memorandum:
Characteristics of Joints at the Santa Susana Field Laboratory, Simi, California

DRAFT

Date: December 10, 2009

Prepared for:

THE BOEING COMPANY
THE NATIONAL AERONAUTICS AND SPACE ADMINISTRATION
THE UNITED STATES DEPARTMENT OF ENERGY

Prepared by:

J.R. Wagner[1] and M. Perkins[2]

[1]Independent Professional Geologist

[2]University of Utah, Salt Lake City, Utah

TABLE OF CONTENTS

LIST OF TABLES

LIST OF FIGURES

LIST OF FIGURES (Continued)

1.0 INTRODUCTION

A joint is a particular kind of fracture in rock. A fracture is a surface of discontinuity in rock with three basic characteristics: (1) it consists of two near parallel surfaces that meet at the fracture front; (2) these surfaces are approximately planar; and (3) the relative displacement of originally adjacent points across the fracture is small compared to fracture length (Pollard and Segall, 1987). Broadly speaking a joint is a mode I or opening displacement fracture (Pollard and Aydin, 1988). An opening displacement fracture is a fracture formed by opening perpendicular to the fracture surfaces. Joints are commonly planar but can be curved or consist of connecting planar and curved segments along their trace. Joints are primarily generated by extensional stresses in rock masses, and since the state and orientation of stress in a rock can vary over geologic time, there are typically joints with two or more orientations in a rock mass.

The Santa Susana Field Laboratory (SSFL) is primarily underlain by the Chatsworth Formation, a Cretaceous age (~80-65 million years old) unit of layered marine sedimentary deposits. It comprises a sequence of ~8000 ft of indurated Cretaceous sandstone, shale, and minor conglomerate. As is typical of indurated and layered sedimentary units, joints are a pervasive feature of the Chatsworth Formation at the SSFL. The purpose of this report is to present the findings on the characteristics of the joints observed in surface outcrops of the Chatsworth Formation in and around the SSFL.

2.0 FIELD OBSERVATIONS

2.1 JOINT ORIENTATION MEASUREMENTS

Three groups of joint orientation measurements were collected in Chatsworth Formation sandstone in the SSFL area. Emphasis was placed on sandstone of the Chatsworth Formation for two reasons: first, because it is the dominant rock type in this formation and is well-exposed in many areas: and second, because shale, the other common rock type, is generally not well-exposed.

The first group of orientation measurements consists of outcrop measurements using a Brunton™ type geologic compass. These ~220 compass measurements include both the trend (strike) and inclination (dip) of the joint surfaces. They are listed **Table 1**. The 3-D orientations of the compass measurements are shown graphically on the stereonet of Figure 1. The spatial distribution of the trends of these measurements is shown graphically with "rose" diagrams on **Figure 2**. The second group of orientation measurements consists of trends of ~460 joints visible on aerial photographs in the northern SSFL. These trends were measured with a protractor. These trends are summarized in **Table 2** and also shown with rose diagrams in **Figure 2**. Finally, a third group of orientation measurements consists of trends and lengths measured on Google-Earth™ imagery. These ~ 300 trends and length measurements are listed in **Table 3** and their spatial variation is illustrated with the "star" diagrams in **Figure 3**.

All joint orientation measurements are subject to some measurement error. Observations at outcrops show joint surfaces can be irregular in detail. So a measurement with compass at a particular locality will include both the error of the compass measurement at that locality (~±2-4º) and the deviation of a joint surface at a particular locality from the overall average orientation of the joint. This deviation is not well established but may be in the range of ±5-10º. For measurements of joint trends on the aerial photographs and Google Earth™ imagery (also based on aerial photography in the site area), observed surface traces of non-vertical joints will only parallel the strike of a joint surface if the ground is level and the focus of the camera is vertical.

The first of these conditions is not generally met at the SSFL and there are likely deviations from the second condition as well. Expected deviations of joint traces from joint strike directions due to joint inclinations and topographic slope may range up to 20-30º or more. A deviation as large as 30º occurs only for joints with dips of 60º and slopes that trend normal to the strike of a joint and slope 30º. Most measured joins dip >60º and most slopes are not normal to joint strikes and incline less than 30º. So deviations of measured trends on aerial photographs from actual joint strikes will commonly be less than 30º.

Figure 1 shows essential characteristics of the SSFL joint orientations. First, joints are mostly steeply dipping with only 27 joints (12%) dipping less than 60º and only 4 joints (2%) dipping less than 30º. Second, the steeply dipping joints fall into two dominate clusters termed the NE striking set and the NW striking set. Third, the NE joint set strikes sub parallel to bedding and, on average, dips steeply SE intersecting bedding and an angle of ~75º. Fourth, the NW joint set strikes ~90º to bedding strike, dips steeply SW, and intersects bedding at an average angle of ~90º. Finally, about 70 (32%) of the measured joints fall outside of the main fields of the NE and NW striking joint sets, that is, outside of the contoured areas. This set of joints, the “low density” set are broadly distributed in strike, dip ~60º on average, and generally have densities <2%/unit area. All these essential characteristics of the SSFL joints are summarize in the **Figure 5** block diagram which shows the joint orientations relative to a hypothetical sandstone bed.

2.2 SPATIAL PATTERNS OF JOINT ORIENTATIONS AND ORIENTATION FREQUENCY

2.2.1 Area Wide Patterns

The two principal joint sets, the NE and NW trending sets, while recognizable throughout the SSFL area, show variability in both relative abundance of joints between the two sets and the mean trend of each set from location to location. In **Figure 2** the rose diagrams show the joint trends and their variation throughout the SSFL area. The joint trends measured on aerial photos, available only for the northwestern SSFL, fall distinctly into either the NW set or the NE set. The joint trends measured with compass also show concentrations in these two sets but these concentrations are more diffuse and imbedded in a “haze” of joints in the “low density” set. The

contrast between the two data sets may reflect both measurement bias and spatial variation in the relative proportion of the “low density” joints. With aerial photographs only the longer joints are visible. In contrast joints measured by compass at outcrops include joints of all lengths.

Analysis of Google Earth™ imagery yields joint trend distributions similar to those revealed by the aerial photo analysis but on a more detailed spatial grid (**Fig. 3**). These measurements are displayed using “star” diagrams which show both the trend and length of individual measurements in each grid cell. As with the measurements of **Figure 2**, those of **Figure 3** show the NW joint set dominant in the northwest area with an eastward increase in the relative abundance of the NE joint set. Because of sparse outcrops south of the Burro Flats Fault measurements on Google Earth™ imagery were not carried out in this area.

2.2.2 Local Patterns

The graphical plots of joint orientations discussed above provide an understanding of dominant directions and the variations and similarities of average joint directions from area to area. Imagery, however, provides more detail than can be captured with graphical plots. Below, some of the variation in joint patterns from area to area is discussed and illustrated with Google Earth™ images and field photographs. The locations of the Google images are shown on **Figure 5** and descriptions of observed patterns are discussed below.

Unimodal Joint Pattern The simplest joint pattern in the Chatsworth sandstone is that of joints with a single trend (unimodal joint pattern). Such a pattern is characteristic of the thick sandstone in the uppermost part of the Chatsworth Formation exposed along the northern perimeter of the SSFL. Here, as shown on **Figure 6**, the thick sandstone beds have a well-developed set of NNW joints. The sandstone here forms a dip slope (a slope parallel to the bedding dip) and the joints trend down-dip with visible lengths up to 400 ft and with a few visible joints oriented ENE across this trend. Field photo MP4219 (**Fig. 7**) shows a ground view of this dip slope from the north.

Orthogonal Joint Pattern A more common pattern of Chatsworth sandstone jointing is that of two dominant trends at ~90° to one another. Such a pattern is seen in the thick bedded sandstone

outcrops to the northeast of the SSFL north of Woolsey Canyon Road. This area is shown in the **Figure 8** Google Earth™ image and another view is shown in field photo MP4200 (**Fig. 9**). In the **Figure 8** area, exposed on bare dip slopes, joints trend both ENE parallel to bedding strike and NNW in the down dip direction.

Similar orthogonal joint patterns are seen elsewhere in and around the SSFL, as shown on the Google Image of **Figure 10**. Here, along the southern perimeter of the SSFL, exposures are less complete, but nevertheless the orthogonal joint pattern is evident with one joint set trending NNE parallel to bedding in this area and the second set trending WNW normal to the first set in the dip direction.

Variable Joint Patterns Less uniform joint patterns are also common. One example is evident in the Google Earth™ image of the area around the main office of the SSFL. Here (**Fig. 16**) is a patchwork or mosaic distribution of joint trends in the Chatsworth sandstone. Just east of the office (arrows "**a**"), joints of the NW set are prominent and are expressed by the dark linear elements traversing light colored sandstone outcrops. In detail these joints are not parallel, as they might be in a simple set, but instead form a radiating pattern from NW on the east to N on the west. To the west and south of the office this pattern gives way to a less organized mix of NW and NE joints of varying direction and spacing along with joints of more random orientation.

Another area of variable joint patterns is seen in the Google Earth™ image of **Figure 17** which is located ~1 km N30W from the center of the **Figure 8** image. On the dip slope in the western third of the image, a simple orthogonal joint pattern is seen with most joints trending NNW in the down dip direction. A secondary set, orthogonal to the first, is trending ENE approximately parallel to bedding strike. A second, more complex orthogonal joint pattern is evident on the dip slope in the central part of the image. Here, joints are curvilinear rather than linear with a NNW set of joints appearing to curve southward into an ENE set.

2.3 JOINT SPACING/DENSITY

Joint spacing as well as joint orientation shows spatial variation. The spacing between joints is the average spacing between joints in the direction perpendicular to the trend of a joint set. It can also be expressed as a density, i.e., the number of joints in a given length perpendicular to trend of a joint set. In areas with good exposure, joint spacing/density can be measured on aerial photographs and on Google Earth™ images. Such exposures are common north of the Burro Flats Fault and joint spacing/density in the Chatsworth sandstone of this area was measured on aerial photographs and is summarized in **Figure 18**. Note, however, that measured values do not include joints below the resolution of the imagery. Thus, the measured joint spacings are maximum values and, conversely, the densities are minimum values.

Figure 18 shows the joint spacing measurements from these photos with the equivalent joint density values (number of joints/100 ft) shown by the color coding. These density values show considerable variation ranging from less than 0.5/100 ft to greater than 4/100 ft. The 1st order pattern shows lowest densities mostly to the west and along the northern SSFL boundary with higher densities concentrated to the east. Spot measurements of joint density have been made on a number of Google Earth™ images in the area of the **Figure 18** measurements and areas to the NE in equivalent strata. Examples of these measurements are shown on several figures and their captions (see **Figs. 6, 8, 10, 16, 17, 19, 20, 21**). These measures indicate the local variation in joint density can be as great as the area wide densities shown on **Figure 18**.

Outside of the **Figure 18** measurement area, that is the area to the south of the Burro Flats Fault and the area to the east of the "shear zone" that is mapped, exposures of Chatsworth sandstone are limited. Nevertheless, field observations and the examination of Google Imagery indicate that joint densities are commonly higher than found in the **Figure 18** area. **Figure 10** shows one such high joint density area along the southern boundary of SSFL. As shown on this figure densities of ~4.0 to as high as 10 are typical. In contrast only 11% of the measurements in the Upper Chatsworth sandstone have densities above 4.0 (**Fig. 18**).

2.4 JOINT LENGTH

In the survey of orientations of prominent joints visible on Google Earth™ imagery (**Fig. 3**) measurements of lengths were also recorded (**Table 3**). Almost all of these lengths represent minimum lengths of the measured joints because the joints extend beyond the boundary of the outcrop, and hence the actual joint terminations are rarely exposed. Measured lengths, all of which are the horizontal projections of ground lengths, range from ~ 50 to 1000 ft. Of these measured lengths 88% are in the range of 100 to 400 ft. Without question there are numerous joints of less than 50 ft of visible length, but these were excluded from the survey which focused on the trends of the more prominent, longer joints. In outcrops joints commonly extend along the full outcrop length but shorter joints do occur. Examples of such joints are shown in a field photo 4103 (**Figs. 22, 23**). Little can be said about either the full range of joint lengths or the possible distribution law controlling joint lengths. However available information suggests that many joints may be as short as a few 10's of feet and that at least a few can be in excess of 1000 feet.

2.5 JOINT HEIGHT

2.5.1 Within Sandstone Beds

With bedding as a reference surface joint height here refers to the dimension of a joint in the direction normal to bedding. In the Chatsworth sandstone some joints are quite short and don't cross the full thickness of a bed. More commonly others cross the full thickness of either a single bed or an amalgamation of several sandstone beds. A single bed can be as thin as a few centimeters or as thick as 10 meters or more. Amalgamations of sandstone beds can be thicker still.

Figure 22 shows an exposure of an amalgamated sandstone layer just north of the Burro Flats Fault. The left (eastern) side of this outcrop follows an ENE trending SSE dipping joint that traverses the entire thickness of this amalgamated bed. This "master" joint is evident on detailed Google Earth™ views. The other joints seen in **Figure 22** all parallel the "master" joint but are not expressed in Google Earth™ views. Some of less well expressed joints also traverse the entire thickness of the exposure, but others appear to fade out downward in the bed (see joint marked by arrow "**j**" in **Fig. 22** and others seen in detail in **Fig. 23**). This "fading out" may be a

consequence of differential weathering with joints becoming wider and more visible as they approach the upper surface of the outcrop.

Figure 24 shows thick bedded, often amalgamated sandstone layers exposed just north of the Burro Flats Fault. While these beds have not been examined closely, the joint heights seem to be limited to either the height of individual beds or amalgamations of several beds. Also, joint spacing appears to be roughly proportional to bed/amalgamated beds thickness with relatively close spacing seen in the thinner beds on the right side of the sandstone outcroppings and much wider spacing in the very thick (~40 – 60 ft) beds to the left. Such a linear relationship of joint spacing to bed thickness is a common feature in layered sedimentary rocks. The possible implication of this relationship to joint connectivity will be brought up in closing discussions.

2.5.2 Control by Shale Beds

While shale is a minor component of the Chatsworth Formation, particularly the upper parts of the Chatsworth Formation underlying SSFL, it may exert a strong control on joint height. While exposures of relatively unweathered shale are limited, several that have been examined commonly contain thin sandstone beds. These sandstone beds, shown in **Figure 25**, are finely jointed and the joints terminate at the shale/sandstone contacts. A more striking example of this is seen in a deep excavation for water tanks along the southern perimeter of the SSFL. Here (**Figs. 10, 11, 12, and 13**) are thick sandstone beds with some very thin shale interbeds (~0 – 0.5 ft) and one ~3 ft thick bed of interbedded shale and thin sandstone. As shown in the photographs in **Figures 12 and 13**, well developed joints in underlying sandstone terminate at the shale/ thin bedded sandstone contact. Elsewhere in this water tank cut some joints in the sandstone extend through the thin shale interbeds while others traverse these interbeds.

2.6 JOINT CONNECTIVITY

Joint connectivity within beds and across beds can be assessed locally in areas of good exposures of the Chatsworth Formation. In areas with dip slope exposures, the lateral connectivity within a bed is displayed. In areas with vertical exposures, the connectivity normal to bedding is displayed. Examination of these exposures in the field and on Google Earth™ imagery across the SSFL area suggests variability in the intensity/density of joint intersections in sandstone beds, and, by inference, variability in joint connectivity. Observations on such variability in potential joint connectivity in various rock types and geologic contexts are discussed below.

2.6.1 Well-Jointed Sandstone

Throughout much of the SSFL areas, two or more sets of intersecting joints are well developed. Several such areas are shown in **Figures 8, 11, 16, 19, and 20**. In such areas joints likely form a connected network.

In other areas the density of intersections appears to be more limited. In such areas the degree of connectivity may be more limited. One such area with good exposures is in the NW SSFL. Here, the thick sandstone beds of the upper Chatsworth display only one well-developed ~~systematic~~ joint set, the NW set. As shown in several figures (**Figs 3, 18, 21, and 26**), these joints are widely spaced. In the thick bedded sandstone somewhat further to the south, joints of varying strike are more common, but within individual beds or amalgamations of beds only one joint direction is typically well expressed (**Figs. 6, 19, and 20**). In such areas vertical connectivity may be limited but joints may be connected laterally within individual beds..

2.6.2 Sparsely Jointed Sandstone

The thick bedded sandstone of the upper Chatsworth Formation underlies the NW portion of the SSFL north of the Burro Flats Fault. This area, as shown on **Figure 18**, is characterized by low joint density in many places. Furthermore, joints in individual sandstone beds often have only one pronounced joint set, the NW trending set, with other joint directions either absent or weakly developed (**Figs. 6, 9, 20, and 26**).

2.6.3 Mismatched Joints in Sandstone

Another characteristic of the sparsely-jointed sandstone is the mismatch of joint orientations from layer to layer. Examples of this are shown in **Figure 21**. This mismatch suggests that there are layers between individual beds of sandstone that have limited the propagation of joints from layer to layer. These layers may be separated by thin shale or some other layer resistant to joint formation. Such a mismatch in joint orientation may limit connectivity from bed to bed.

Another type of mismatch is joint density mismatch. An example of such a mismatch is seen in **Figure 16**. Here the trend of the dominant joint set is parallel from bed to bed but thinner beds have higher joint densities. This again suggests a thin layer between beds, possibly shale, is limiting joint propagation from sandstone to sandstone with each sandstone bed jointing independently of other sandstone beds. Again, the bed to bed mismatch may limit connectivity from bed to bed.

2.6.4 Shale Interbeds

Units of shale are a minor but important component of the Chatsworth Formation. Thick units, commonly of considerable extent, are present in the SSFL area. Thinner units, ranging in thickness from a few centimeters to several meters are also seen in outcrops throughout the SSFL area. As noted previously, joints within these shale layers appear to be restricted to the thin sandstone interbeds that are common in the shale units (**Fig. 25**) and joints extending fully across thick shale units may be absent or, at most, widely spaced. The resistance of shale to jointing reflects the strong contrast in mechanical properties between the sandstone and shale. The excellent water tank exposure, also discussed previously, provides vivid examples of well-developed joints in Chatsworth sandstone terminating at a 1 m thick shale unit (**Figs. 12 and 13**). In contrast, thin (< 0.2 m), lenticular shale layers in the this exposure provide more limited impediment to joint propagation with some joints terminating at the boundaries of these thin shale layers and others extending through these thin layers.

3.0 SUMMARY

As shown by field investigations of surface outcrops and by interpretation of aerial photography and Google Earth™ imagery joints are a pervasive structural feature of sandstone beds in the Chatsworth Formation that underlies the SSFL. The measurements of the trends of ~1000 joints indicate that most (~70%) joints belong to one of two sets, a NW trending set and a NE trending set. Examination of outcrops shows that joints in these two sets are steep dipping (>60°). Other joints, lying outside the spatial field of these joints, are mostly relatively steep dipping as well (>50°). Only a few (~2%) low dipping joints (<30°) were observed in outcrops.

Analysis of imagery shows that exposed Chatsworth Formation sandstone commonly contains an array of variable trending high angle joints, with the NE and NW sets dominating in most areas. These high angle joints are of sufficient length and density that intersections are frequent allowing the formation of connected networks within individual beds or amalgamated groups of beds. Locally, in the NW part of SSFL where thick sandstone beds are common, only a single joint set, the NW set, is seen in imagery. These joints are widely spaced and may not be well connected. In this area connectivity might be enhanced by the low angle joints, but such joints are not detectable in the imagery examined.

Shale layers are present in the Chatsworth Formation and observations indicate that high angle joints terminate at thick shale units (>3 ft). Thus, bed to bed connectivity of joints in areas of shale is likely limited, but connectivity along bedding is still feasible.

All of the above observations indicate that joints likely form connected networks over much of the SSFL. However, local conditions may limit connectivity such as, shale beds limiting bed to bed connectivity and sparsely jointed areas or areas with only a single joint set having little or no connectivity if low angle joints are lacking.

4.0 REFERENCES

Pollard, D.D. and Segall, P., 1987, Theoretical displacement and stresses near fractures in rock: with applications to faults, joints, veins, dikes, and solution surfaces: *in* B.K. Atkinson, ed., Fracture Mechanics of Rock, Academic Press, Inc., pp. 277-349.

Pollard, D. D. and Aydin, A., 1988, Progress in understanding jointing over the past century: Geological Society of America, v. 100, p. 1181–1204.

TABLE 1. SSFL JOINTS: BRUNTON COMPASS MEASUREMENTS

Domain	Strike	Dip	Lat	Long	Domain	Strike	Dip	Lat	Long	Domain	Strike	Dip	Lat	Long
D0	N12W	76W	34.22182	-118.70457	D2/3	N75W	68E	34.21425	-118.69642	D3	N5E	71E	34.21609	-118.69025
D0N	N70W	70N	34.22611	-118.71184	D2/3	N30E	78E	34.21425	-118.69642	D3	N75W	53N	34.21502	-118.69022
D0N	N20W	15E	34.22611	-118.71184	D2/3	N10E	65E	34.21430	-118.69713	D3	N62E	75S	34.21455	-118.69080
D0N	N60W	60E	34.22143	-118.68772	D2/3	N85E	78N	34.21430	-118.69713	D3	N80W	90E	34.21438	-118.69204
D0N	N25E	73E	34.22307	-118.68370	D2/3	N45E	76N	34.21624	-118.69394	D3	N55W	70N	34.21574	-118.69217
D0N	N85E	55S	34.22307	-118.68370	D2/3	N74E	80S	34.21613	-118.69383	D3	N45E	63S	34.21768	-118.69475
D0N	N85E	17N	34.22307	-118.68370	D2/3	N78W	80N	34.21593	-118.69383	D3	N70W	75S	34.21799	-118.69512
D0N	N68W	85W	34.22307	-118.68370	D2/3	N25E	63E	34.21513	-118.69278	D3	N28W	73E	34.21817	-118.69443
D0N	N70W	77S	34.22348	-118.68251	D2/3	N80W	90E	34.21465	-118.69357	D3	N38E	82W	34.21860	-118.69448
D0N	N85E	85S	34.22348	-118.68251	D2/3	N60E	69S	34.21446	-118.69377	D3	N40W	85W	34.21880	-118.69437
D0N	N55W	62E	34.22348	-118.68251	D2/3	N55E	75N	34.21328	-118.69463	D3	N39E	85E	34.21894	-118.69445
D0N	N35W	90E	34.22348	-118.68251	D2/3	N0W	90E	34.21454	-118.69707	D3	N16E	76W	34.21902	-118.69457
D0N	N35E	80E	34.22348	-118.68251	D2/3	N85W	85N	34.21432	-118.69811	D3	N48W	88N	34.21881	-118.69509
D0N	N80W	62S	34.22292	-118.68169	D2/3	N80W	57S	34.21390	-118.69841	D3E	N80E	90E	34.21799	-118.68218
D0N	N20E	60W	34.22336	-118.67965	D2/3	N24E	80E	34.21365	-118.69862	D3E	N25W	72E	34.21759	-118.68240
D0N	N35W	75W	34.22336	-118.67965	D2/3	7E	67E	34.21297	-118.69901	D3E	N60E	85N	34.21714	-118.68242
D0N	N10E	70W	34.22271	-118.68042	D2/3	N85W	85N	34.21288	-118.69966	D3E	N50W	85S	34.21700	-118.68161
D0N	N5E	50W	34.22271	-118.68042	D2/3	N45E	50N	34.21259	-118.69981	D3E	N55E	82N	34.21687	-118.68140
D0N	N40W	55W	34.22271	-118.68042	D3	N35W	90W	34.22124	-118.68900	D3E	N80W	77S	34.21798	-118.67822
D0N	N55E	50E	34.22199	-118.68056	D3	N5E	80W	34.22124	-118.68900	R1	N78W	75S	34.234	-118.700
D0N	N70W	77S	34.22343	-118.68234	D3	N65W	88E	34.22124	-118.68900	R1	N34W	84S	34.234	-118.700
D0N	N60W	73N	34.22295	-118.68140	D3	N20E	90W	34.22124	-118.68900	R1	N14W	86E	34.234	-118.700
D0N	N80W	72S	34.22282	-118.68125	D3	N76W	50W	34.22124	-118.68900	R1	N54E	77S	34.234	-118.700
D0N	N20E	60W	34.22288	-118.68044	D3	N35E	90W	34.22124	-118.68900	R1	N52W	84N	34.234	-118.700
D0N	N35W	75S	34.22302	-118.68014	D3	N80E	83S	34.21903	-118.68947	R1	N35W	57N	34.234	-118.700
D0N	N55E	50S	34.22216	-118.68025	D3	N80E	83S	34.21903	-118.68947	R1	N68W	80S	34.234	-118.700
D0N	N75W	60S	34.22200	-118.68051	D3	N0W	90W	34.21626	-118.68896	R1	N27E	72E	34.234	-118.700
D0N	N45W	65S	34.22295	-118.68945	D3	N20E	90W	34.21626	-118.68896	R1	N40W	90W	34.234	-118.700
D0N	N10E	75E	34.22253	-118.68971	D3	N50E	73E	34.21626	-118.68896	R1	N42W	83S	34.234	-118.700
D0N	N28E	75E	34.22226	-118.68953	D3	N43E	65E	34.21626	-118.68896	R1	N36E	68S	34.234	-118.700
D0N	N20E	84E	34.22052	-118.68922	D3	N5W	90W	34.21626	-118.68896	R1	N26W	78S	34.234	-118.700
D0N	N40W	71S	34.22135	-118.68790	D3	N35E	78E	34.21626	-118.68896	R1	N29E	73E	34.234	-118.700
D0N	N62E	57S	34.22131	-118.68737	D3	N15E	85E	34.21626	-118.68896	R1	N88W	74S	34.234	-118.700
D0N	N63W	82N	34.22140	-118.68704	D3	N12W	75E	34.21626	-118.68896	R2	N80E	84S	34.213	-118.780
D0N	N0W	90W	34.22162	-118.68469	D3	N15W	75W	34.21626	-118.68896	R2	N41E	83N	34.213	-118.780
D0N	N75W	90E	34.22162	-118.68469	D3	N5E	60E	34.21626	-118.68896	R2	N41E	68S	34.213	-118.780
D0N	N40E	65E	34.22682	-118.71158	D3	N5W	85W	34.21626	-118.68896	R2	N51W	73S	34.213	-118.780
D1	N80W	80S	34.22326	-118.70748	D3	N50W	85E	34.21626	-118.68896	R2	N59W	88S	34.213	-118.780
D1	N50E	75E	34.22326	-118.70748	D3	N45E	88W	34.21626	-118.68896	R2	N9E	90W	34.213	-118.780
D1	N60W	80N	34.22052	-118.70683	D3	N90W	82S	34.21626	-118.68896	R2	N18W	75W	34.213	-118.780
D1	N70E	48S	34.22052	-118.70683	D3	N75W	80S	34.21626	-118.68896	R2	N37W	86W	34.213	-118.780
D1	N70E	58N	34.22052	-118.70683	D3	N43W	90W	34.21626	-118.68896	R2	N31W	73N	34.213	-118.780
D1	N0W	70E	34.22038	-118.70782	D3	N65W	47W	34.21626	-118.68896	R2	N86E	88S	34.213	-118.780
D2	N80W	80S	34.21949	-118.69819	D3	N80W	85E	34.21626	-118.68896	R2	N72W	64S	34.213	-118.780
D2	N40W	80W	34.21949	-118.69819	D3	N5W	63W	34.21626	-118.68896	R2	N63W	79S	34.213	-118.780
D2	N55E	53E	34.21949	-118.69819	D3	N50W	85W	34.21626	-118.68896	R2	N35W	84E	34.213	-118.780
D2	N30W	78W	34.21949	-118.69819	D3	N35W	77E	34.21626	-118.68896	R2	N33E	88S	34.213	-118.780
D2	N48E	68E	34.21949	-118.69819	D3	N57W	65W	34.21626	-118.68896	R3	N34W	82E	34.231	-118.656
D2	N63E	87W	34.21949	-118.69819	D3	N70W	80N	34.21626	-118.68896	R3	N18E	74E	34.231	-118.656
D2	N45E	80N	34.21908	-118.69575	D3	N70E	88S	34.21626	-118.68896	R3	N57W	72S	34.231	-118.656
D2	N80E	25N	34.21983	-118.69645	D3	N60W	60E	34.22038	-118.68318	R3	N34E	85S	34.231	-118.656
D2	N45W	65N	34.21713	-118.69685	D3	N67W	73E	34.22038	-118.68318	R3	N37E	82S	34.231	-118.656
D2	N58W	73N	34.21691	-118.69677	D3	N50W	77E	34.22038	-118.68318	R3	N58W	78S	34.231	-118.656
D2	N40W	70E	34.21608	-118.69718	D3	N10E	50S	34.22038	-118.68318	R3	N37E	72S	34.231	-118.656
D2	N75W	78S	34.21524	-118.69916	D3	N80E	80S	34.21701	-118.68157	R3	N12E	84W	34.231	-118.656
D2	N78E	72S	34.21492	-118.69930	D3	N80E	80N	34.21701	-118.68157	R3	N0E	81W	34.231	-118.656
D2	N19E	86E	34.21444	-118.70040	D3	N70E	90E	34.21812	-118.67828	R3	N41W	88N	34.231	-118.656
D2	N57E	54S	34.21706	-118.70135	D3	N63W	75S	34.21778	-118.68332	R3	N39W	76N	34.231	-118.656
D2	N67W	87N	34.21829	-118.70165	D3	N25E	85E	34.21793	-118.68353	R3	N53E	86S	34.231	-118.656
D2	N70W	55N	34.21840	-118.69982	D3	N38E	58W	34.21910	-118.68373	R3	N63E	74S	34.231	-118.656
D2	N72W	70S	34.21713	-118.70261	D3	N80W	90E	34.21938	-118.68358	R3	N54W	80N	34.231	-118.656
D2	N45W	90E	34.21700	-118.70276	D3	N10W	83E	34.21955	-118.68368	R3	N2E	63W	34.231	-118.656
D2	N90W	80S	34.21689	-118.70301	D3	N28E	80E	34.21988	-118.68349	R4	N23E	79W	34.223	-118.661
D2	N65W	88S	34.21666	-118.70319	D3	N32W	62W	34.21939	-118.68452	R4	N51W	75E	34.223	-118.661
D2	N40E	77E	34.21679	-118.70362	D3	N10W	37W	34.21949	-118.68481	R4	N17E	86E	34.223	-118.661
D2	N33E	90E	34.21945	-118.70263	D3	N22W	77W	34.21945	-118.68498	R4	N67E	83W	34.223	-118.661
D2	N20E	78E	34.22020	-118.70340	D3	N25E	85E	34.21640	-118.68762	R4	N9W	73E	34.223	-118.661
D2	N12W	74E	34.22075	-118.70361	D3	N30E	13W	34.22119	-118.68347	R4	N19E	79E	34.223	-118.661
D2	N75W	80S	34.22198	-118.70631	D3	N45E	77N	34.21896	-118.69000	R4	N32E	87W	34.223	-118.661
D2	N65W	80S	34.22036	-118.70590	D3	N63E	62N	34.21800	-118.68936	R4	N54W	87E	34.223	-118.661
D2	N3E	66E	34.21846	-118.70480	D3	N58E	85S	34.21774	-118.68942	R4	N54E	79W	34.223	-118.661
D2	N48W	75N	34.21826	-118.70522	D3	N20W	55W	34.21726	-118.68951	R4	N58W	83E	34.223	-118.661
D2	N53W	57S	34.21766	-118.70513	D3	N55E	52S	34.21638	-118.69031	R4	N59W	73E	34.223	-118.661
D2	N90W	90E	34.21698	-118.70516	---	---	---	---	---	---	---	---	---	---

Note: Domains are areas of measurements. In domains D0, D0N, D1, D2, D3, and D3E the Lat and Long is the measurement location while in domains R1, R2, R3, and R4 the Lat and Long is the location in the central part of the domain. See Figure 2 for domain locations and rose diagrams showing patterns of strike orientations in domains.

TABLE 2. SSFL JOINTS: AIRPHOTO STRIKE MEASUREMENTS

Domain	Strike Interval	Num.	Domain	Strike Interval	Num.	Domain	Strike Interval	Num.	Domain	Strike Interval	Num.	Domain	Strike Interval	Num
R5	N80-70W	1	R6	N90-80W	4	R7	N90-80W	1	R8	N90-80W	1	R9	N90-80W	4
R5	N70-60W	2	R6	N50-40W	14	R7	N80-70W	2	R8	N20-10W	27	R9	N70-60W	4
R5	N60-50W	7	R6	N40-30W	6	R7	N70-60W	3	R8	N10-00W	31	R9	N60-50W	7
R5	N50-40W	8	R6	N00-10E	7	R7	N60-50W	1	R8	N00-10E	6	R9	N50-40W	13
R5	N40-30W	10	R6	N30-40E	1	R7	N40-30W	8	R8	N30-40E	5	R9	N40-30W	4
R5	N30-20W	16	R6	N40-50E	1	R7	N20-10W	5	R8	N50-60E	19	R9	N30-20W	16
R5	N20-10W	13	R6	N80-90E	2	R7	N10-00W	9	---	---	---	R9	N20-10W	36
R5	N10-00W	6	---	---	---	R7	N00-10E	22	---	---	---	R9	N10-00W	45
R5	N00-10E	3	---	---	---	R7	N10-20E	27	---	---	---	R9	N00-10E	11
R5	N10-20E	1	---	---	---	R7	N20-30E	7	---	---	---	R9	N30-40E	17
R5	N30-40E	1	---	---	---	R7	N40-50E	2	---	---	---	R9	N50-60E	21
---	---	---	---	---	---	R7	N50-60E	2	---	---	---	R9	N60-70E	2
---	---	---	---	---	---	R7	N60-70E	1	---	---	---	---	---	---
---	---	---	---	---	---	R7	N80-90E	1	---	---	---	---	---	---

Note: See Figure 2 for domain locations and rose diagrams showing patterns of strike orientations in these domains.

TABLE 3. TREND AND LENGTH OF JOINTS MEASURED ON GOOGLE EARTH™ IMAGERY

Cell	Length (ft)	Trend	Cell	Length (ft)	Trend	Cell	Length (ft)	Trend	Cell	Length (ft)	Trend	Cell	Length (ft)	Trend
R1C3	675	N20W	R2C3	266	N31W	R2C6	277	N34E	R3C5	172	N32E	R4C3	121	N68E
R1C3	163	N13W	R2C3	474	N27W	R2C6	154	N34E	R3C5	208	N27W	R4C3	161	N80E
R1C3	221	N20E	R2C3	497	N3W	R2C6	210	N53E	R3C5	67	N37E	R4C3	387	N85E
R1C3	558	N21W	R2C3	948	N2E	R2C6	238	N37E	R3C5	67	N59W	R4C4	154	N90W
R1C3	393	N28W	R2C3	236	N3E	R2C6	165	N42E	R3C5	213	N20W	R4C4	151	N84W
R1C4	499	N54W	R2C3	367	N24E	R2C6	110	N43E	R3C5	259	N34E	R4C4	159	N70W
R1C4	333	N52W	R2C3	319	N89E	R2C6	362	N44E	R3C5	86	N52W	R4C4	121	N66W
R1C4	810	N47W	R2C4	219	N68W	R2C6	152	N49E	R3C5	80	N83E	R4C4	116	N51W
R1C4	433	N34W	R2C4	253	N61W	R2C6	224	N54E	R3C5	51	N45W	R4C4	60	N46W
R1C4	534	N30W	R2C4	189	N47W	R2C6	265	N60E	R3C5	154	N73W	R4C4	154	N21W
R1C4	293	N24W	R2C4	208	N40W	R3C1	338	N84W	R3C5	394	N36E	R4C4	134	N12W
R1C4	275	N18W	R2C4	279	N32W	R3C1	287	N50W	R3C5	211	N73W	R4C4	195	N6E
R1C4	321	N16E	R2C4	179	N25W	R3C1	207	N35W	R3C5	160	N48W	R4C4	187	N8E
R1C4	280	N10W	R2C4	244	N20W	R3C1	343	N23W	R3C5	168	N34E	R4C4	153	N31E
R1C4	427	N24E	R2C4	265	N8E	R3C1	256	N9E	R3C5	127	N57W	R4C4	268	N34E
R1C4	373	N57E	R2C4	154	N33E	R3C1	341	N38E	R3C5	139	N34E	R4C4	258	N34E
R1C5	212	N60W	R2C5	199	N38W	R3C2	249	N54W	R3C5	134	N7W	R4C4	110	N36E
R1C5	180	N56W	R2C5	197	N2W	R3C2	337	N36W	R3C5	98	N37E	R4C4	151	N39E
R1C5	169	N54W	R2C5	178	N3E	R3C2	351	N36W	R3C5	77	N54W	R4C4	244	N40E
R1C5	192	N53W	R2C5	516	N36E	R3C2	327	N35W	R3C5	209	N45E	R4C4	62	N42E
R1C5	171	N36W	R2C5	376	N36E	R3C2	259	N33W	R3C5	120	N74E	R4C4	146	N46E
R1C5	112	N33W	R2C5	315	N62W	R3C2	308	N1E	R3C5	85	N46E	R4C4	110	N46E
R1C5	104	N29W	R2C5	459	N65E	R3C2	352	N26E	R3C5	343	N34E	R4C4	112	N50E
R1C5	94	N24W	R2C5	165	N2E	R3C2	403	N48E	R3C5	173	N44E	R4C4	132	N54E
R1C5	237	N21W	R2C5	190	N21E	R3C2	349	N53E	R3C5	80	N59W	R4C4	100	N54E
R1C5	264	N20W	R2C5	227	N73W	R3C2	299	N53E	R3C5	171	N48E	R4C4	152	N58E
R1C5	139	N19W	R2C5	267	N49E	R3C2	321	N53E	R3C5	93	N65W	R4C4	134	N62E
R1C5	103	N29E	R2C5	135	N3E	R3C2	353	N53E	R3C5	93	N40E	R4C4	215	N67E
R1C5	79	N42E	R2C5	464	N44E	R3C2	338	N58E	R3C5	47	N56W	R4C4	194	N78E
R1C5	53	N43E	R2C5	196	N75W	R3C3	328	N90W	R3C5	139	N31E	R4C4	163	N89E
R1C5	109	N57E	R2C5	141	N5E	R3C3	406	N87W	R3C5	151	N10E	R4C5	112	N68W
R1C6	153	N61W	R2C5	92	N82W	R3C3	186	N51W	R3C5	74	N52W	R4C5	71	N59W
R1C6	67	N48W	R2C5	317	N35E	R3C3	233	N38W	R3C5	70	N63W	R4C5	123	N54W
R1C6	208	N44W	R2C5	306	N40E	R3C3	312	N31W	R3C5	91	N44E	R4C5	71	N39W
R1C6	346	N41W	R2C5	45	N29W	R3C3	248	N10W	R4C1	307	N56W	R4C5	342	N11W
R1C6	175	N38W	R2C5	232	N52E	R3C3	303	N0E	R4C1	327	N9E	R4C5	100	N5E
R1C6	87	N37W	R2C5	374	N89W	R3C3	356	N43E	R4C2	313	N88W	R4C5	175	N29E
R1C6	224	N36W	R2C5	102	N34W	R3C3	282	N43E	R4C2	388	N87W	R4C5	253	N34E
R1C6	123	N36W	R2C5	280	N50E	R3C3	267	N48E	R4C2	296	N75W	R4C5	79	N36E
R1C6	170	N35W	R2C5	105	N40W	R3C3	279	N57E	R4C2	325	N71W	R4C5	157	N37E
R1C6	120	N34W	R2C5	224	N39E	R3C4	204	N84W	R4C2	251	N51W	R4C5	123	N40E
R1C6	133	N33W	R2C5	206	N49E	R3C4	129	N84W	R4C2	208	N42W	R4C5	230	N45E
R1C6	177	N30W	R2C5	267	N41W	R3C4	329	N66W	R4C2	392	N38W	R4C5	77	N46E
R1C6	111	N28W	R2C5	136	N52E	R3C4	382	N63W	R4C2	293	N35W	R4C5	268	N57E
R1C6	298	N28W	R2C5	155	N89W	R3C4	118	N51W	R4C2	239	N32W	R4C5	105	N64E
R1C6	257	N40E	R2C5	197	N43E	R3C4	222	N39W	R4C2	336	N20W	R4C5	126	N65E
R1C6	278	N41E	R2C5	187	N40W	R3C4	192	N34W	R4C2	344	N2E	R4C5	119	N69E
R1C6	222	N46E	R2C5	158	N52E	R3C4	220	N26W	R4C2	377	N6E	R4C5	143	N81E
R1C6	324	N47E	R2C5	92	N55W	R3C4	160	N26W	R4C2	379	N23E	R5C2	204	N9W
R1C6	195	N48E	R2C5	274	N25E	R3C4	109	N15W	R4C2	298	N27E	R5C2	296	N45E
R1C6	180	N51E	R2C6	170	N72W	R3C4	181	N3W	R4C2	269	N49E	R5C3	173	N78W
R1C6	245	N54E	R2C6	210	N70W	R3C4	201	N0E	R4C3	192	N90W	R5C3	156	N62W
R1C6	259	N55E	R2C6	110	N69W	R3C4	104	N0E	R4C3	411	N77W	R5C3	159	N60W
R1C6	411	N55E	R2C6	192	N68W	R3C4	530	N26E	R4C3	392	N68W	R5C3	101	N58W
R1C6	300	N56E	R2C6	137	N66W	R3C4	224	N31E	R4C3	188	N65W	R5C3	142	N50W
R1C6	215	N57E	R2C6	125	N60W	R3C4	340	N36E	R4C3	177	N38W	R5C3	75	N19E
R1C6	213	N61E	R2C6	114	N56W	R3C4	223	N39E	R4C3	138	N35W	R5C3	162	N36E
R2C2	308	N38E	R2C6	179	N54W	R3C4	203	N40E	R4C3	179	N31W	R5C3	131	N44E
R2C2	332	N13W	R2C6	134	N40W	R3C4	271	N41E	R4C3	101	N30W	R5C4	187	N75W
R2C2	393	N18W	R2C6	216	N38W	R3C4	277	N42E	R4C3	170	N25W	R5C4	67	N90W
R2C2	311	N34W	R2C6	122	N30W	R3C4	203	N42E	R4C3	389	N16W	R5C4	188	N16E
R2C2	639	N38W	R2C6	71	N21W	R3C4	277	N43E	R4C3	185	N8W	R5C4	79	N16E
R2C2	376	N42W	R2C6	200	N4W	R3C4	240	N48E	R4C3	150	N2W	R5C4	215	N24E
R2C2	236	N49W	R2C6	201	N5W	R3C4	138	N48E	R4C3	216	N22E	R5C4	64	N34E
R2C3	262	N60W	R2C6	111	N0E	R3C4	208	N81E	R4C3	145	N25E	R5C4	322	N71E
R2C3	280	N44W	R2C6	200	N23E	R3C5	241	N17W	R4C3	312	N39E	R4C3	232	N50E
R2C3	442	N38W	R2C6	181	N30E	R3C5	275	N61W	R4C3	203	N46E	R4C3	206	N53E

Note: See Figure 3 for location of cells and plots of length and orientation measurements..

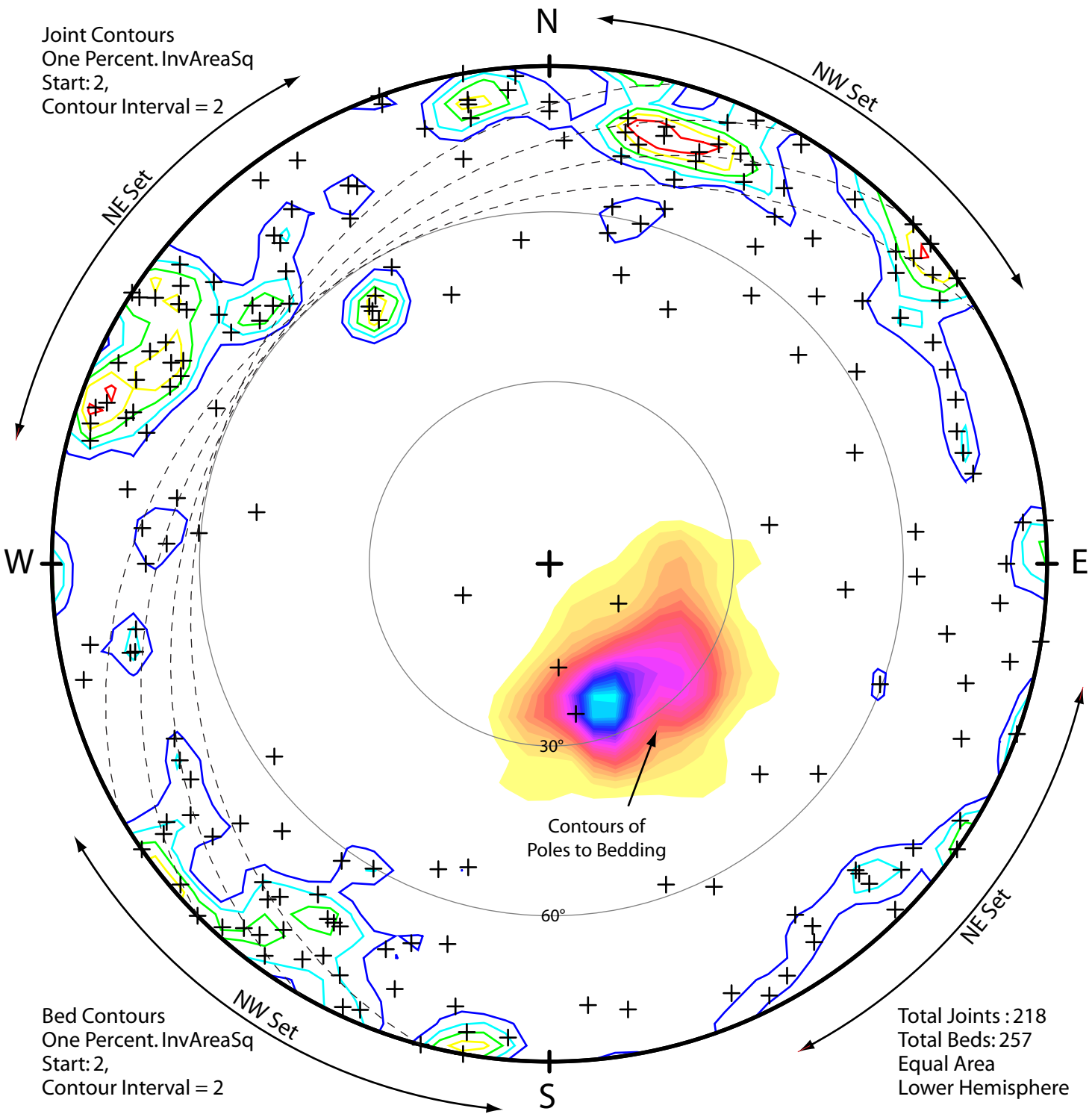

Figure 1. Stereonet plot showing poles to joints and contours of poles to bedding. Poles of joints are marked by "+" symbols. . Poles of the NW striking set of joints are approximately parallel to the strike of bedding. Thus this set of joints is normal to both the bedding strike and bedding plane. Poles to the NE striking set of joints are approximately normal to strike. Thus, this set of joints strike ~parallel to bedding strikeand dips ~normal to bedding. The area that encompasses poles to bedding lies in an area SE of the center of the stereonet. Colors show the density of bedding poles from lowest (yellow) to light blue (highest). The circular contours show the dip of planes represented by plotted poles.

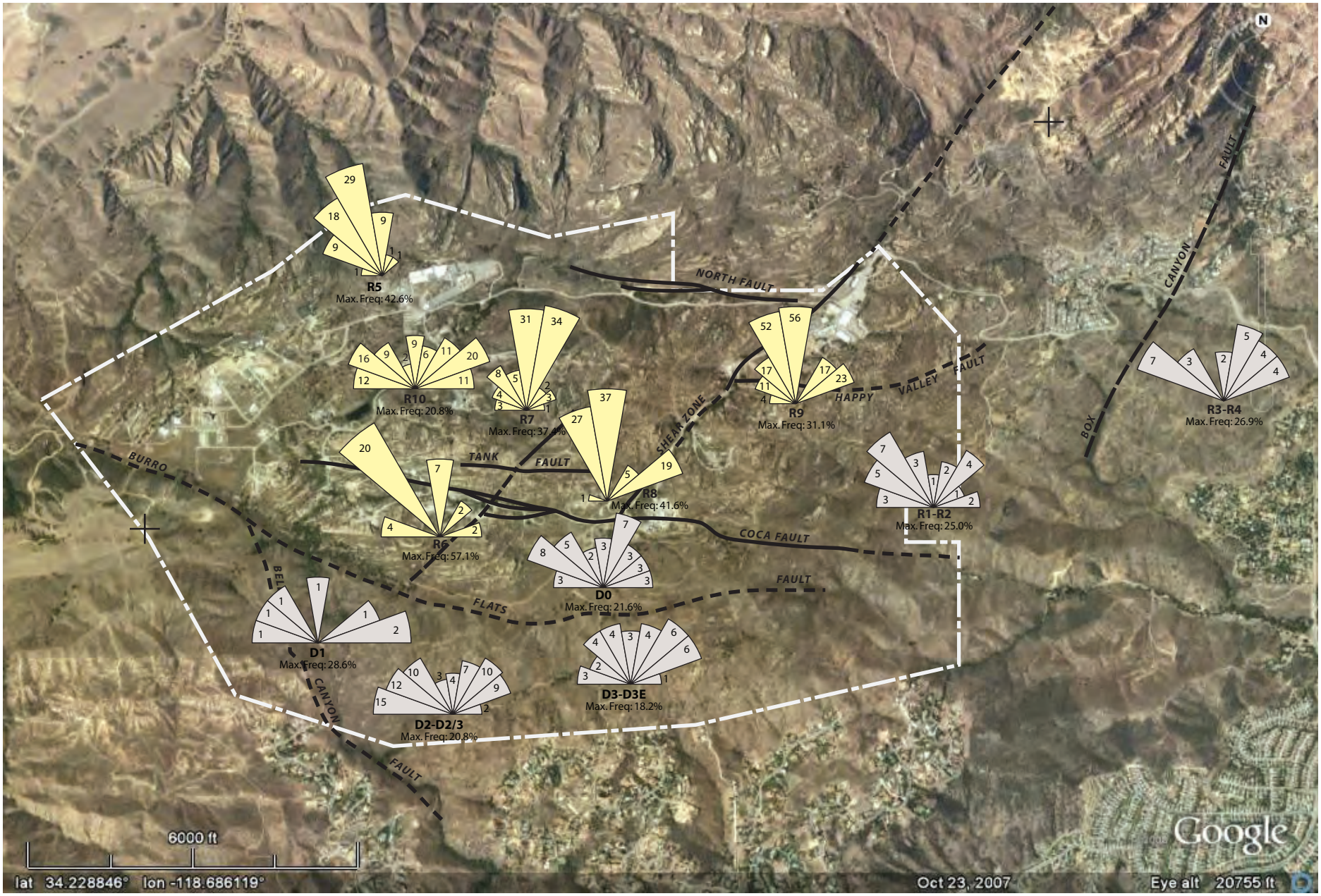

Figure 2. Spatial Distribution of Joint Trends. Rose diagrams with yellow fill are from measurements of trends observed on aerial photographs. Rose diagrams with gray fill are from Brunton compass measurements at outcrops. All measurements are for Chatsworth Fm. sandstone.

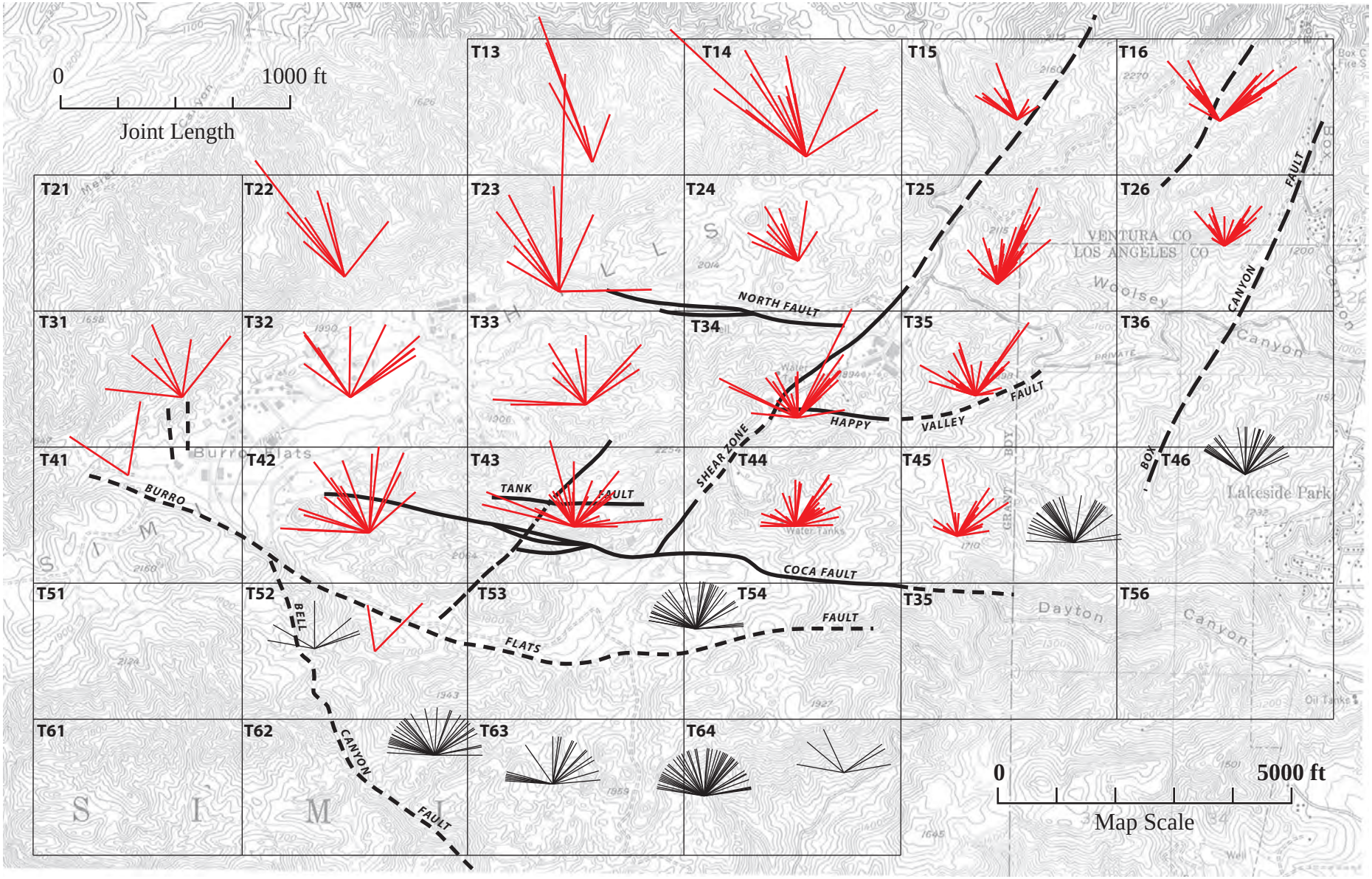

Figure 3. Joint trends in Chatsworth Fm. sandstone. Trends measured on Google Earth imagery (red) with supplemental trends measured by compass (black) in areas with sparse outcrops. For the Google Earth measurements each of the "fan" plots show all measurements within the rectagular grid area (labeled in the upper left corner) with line length proportional to the visible length of the joint (see scale in the NW corner). For tabulation of trends each grid was subdivided into 24 sub-grids (6 wide by 4 high). In the sub-grids the the main trends (mostly 1, sometimes 2 or 3) were measured with 1 measurement per trend. The compass measurements show each strike direction in each of the areas for the rose diagrams in Figure 2. Topography is the from U.S. Geological Survey Calabasas and Simi Valley 1:24,000 quadrangle maps.

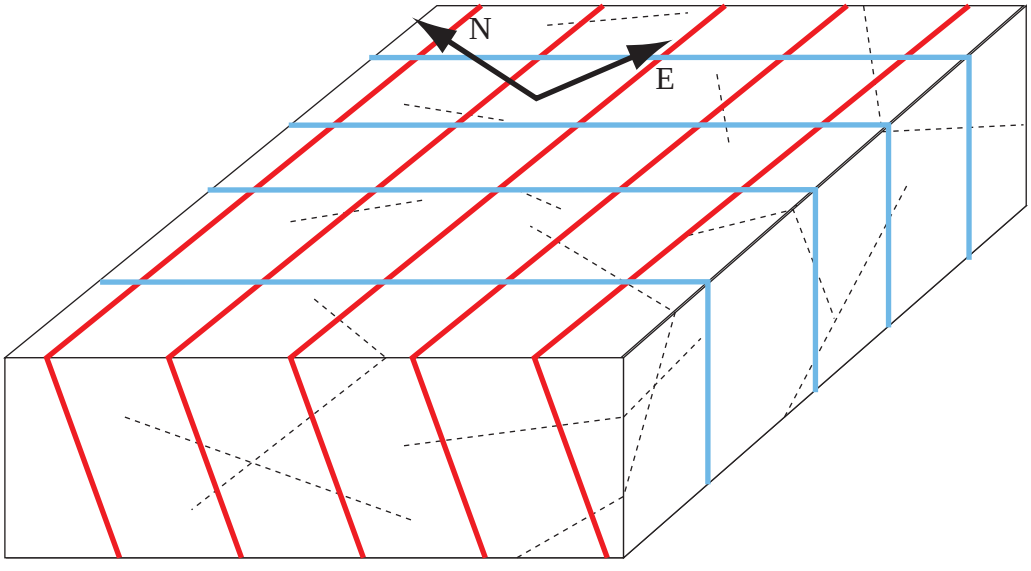

Figure 4. Block diagram showing an idealized model of joint patterns within a Chatsworth sandstone bed. The NE joint set is in red, the NW joint set is in blue, and the “low density” set is marked by dashed lines. The joints are only shown where they intersect the faces of the block diagram.

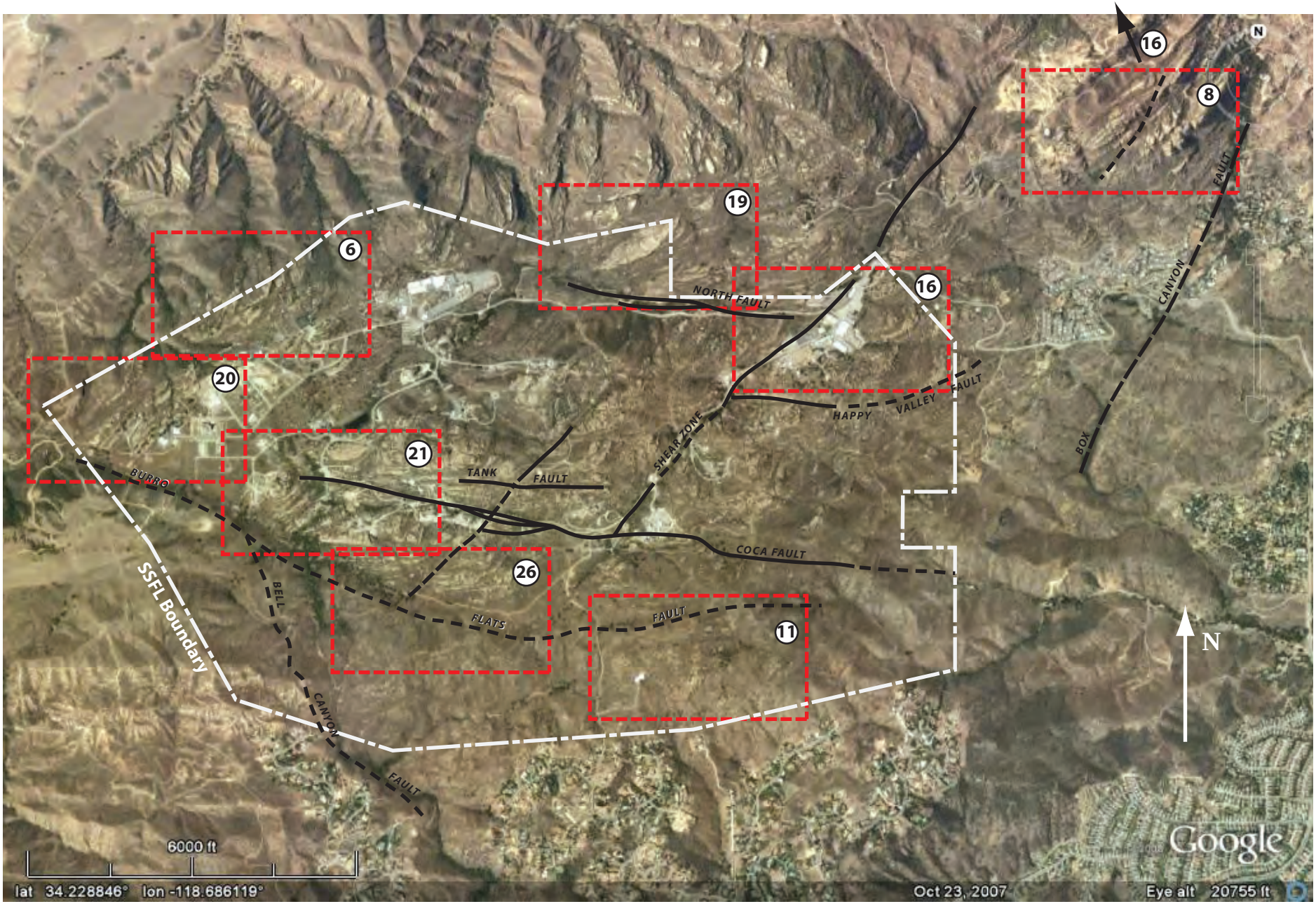

Figure 5. Locations of detailed Google Earth images. Circled numbers are the numbers of the figures showing these images.

Figure 6. Google Earth™ image location 2a (see Fig. 5 for location). This image shows joints in Chatsworth sandstone along the northern boundary of the SSFL. The dominant joint set here strikes NNW. The density of this joint set is ~2.0/100 ft. The arrow labeled “4219” shows the direction of view in field photo MP4219 shown in Figure 7.

Figure 7. Field photo MP4219. View S10E from Meier Canyon towards Chatsworth sandstone along the north boundary of SSFL. This sandstone, with its prominent north trending joint set, is also shown in the Figure 6 Google Earth™ image.

Figure 8. Google Earth™ image location 8 (see Fig. 5 for location). This image shows the joint patterns in the area just west of Box Canyon. Note strong re pattern in the west central part of this Google Earth image. Here the NE trending joints are the best expressed with the NW trending set possibly representing a later set of joints forming between the more dominant NE trending set. The "**a**" arrow points to a bed of Chatsworth sandstone that thickens northeast-ward. Note that the joint density in this bed decreases from ~2.5/100 ft on the west to ~1.1/100 ft on the east where the bed appears to be thicker. The "**b**" arrow points to an ~120 ft thick bed of sandstone with a very low joint density (<0.1/100 ft) in the vicinity of the arrow but with a gradually increasing density southwestward. Possibly this increased density is related to the minor fault (?) crossing the SW end of the thick sandstone bed. The arrow in the lower right corner is the view direction of field photo MP4200 (see Fig. 9).

Figure 9. Field photo MP4200. View N20W from Woolsey Canyon Road towards the very thick, sparsely jointed Chatsworth sandstone. The arrow "**b**" above points to the same sandstone pointed to by arrow "**b**" in Figure 8.

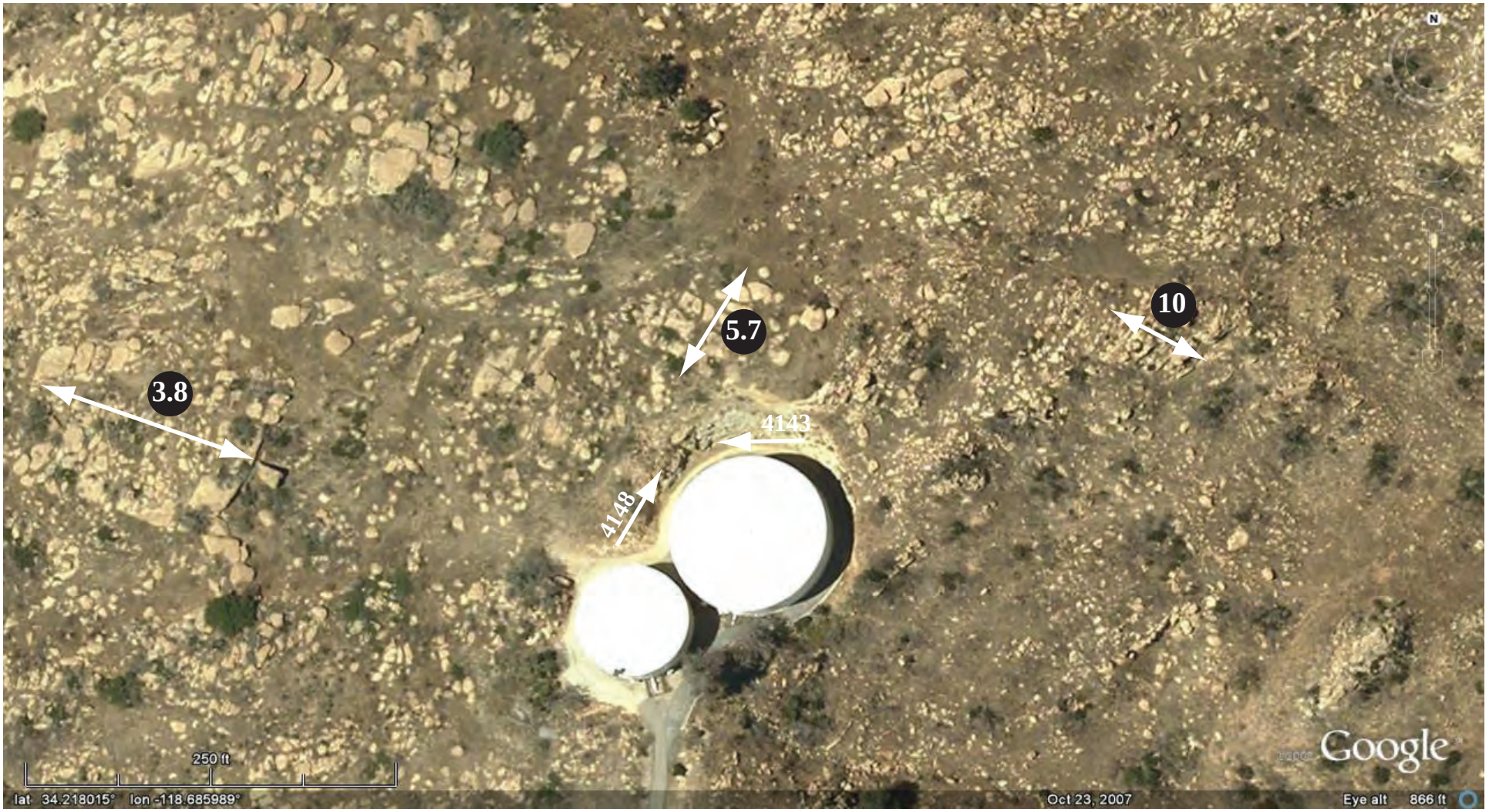

Figure 10. Detailed Google Earth view of Chatsworth sandstone outcrops in the SW 1/4 of Figure 11. The dominant joint trend is ~NNE but note that the lineaments in this direction may also include bedding plane traces. The secondary joint trend is ~WNW and perpendicular to the dominant trend. While joint densities are variable in this area but consistently very high (circled numbers). Exposures in the cut at the north end of the larger water tank provide excellent exposures of the joints and unweathered Chatsworth strata. Field photos MP4143 and MP4148 give overviews of these exposures (see Figs. 12 and 13). The labeled arrows on the image above show the view directions of these field photos.

Figure 11. Google Earth™ image location 11 (see Fig. 5 for location). This image shows the high joint density in this area. The light colored rock is thick-bedded Chatsworth sandstone similar in thickness to sandstone in the central part of photo area 3 with a very low joint density. A more detailed view of the area around the water tanks in the SW corner of this image is shown in Figure 10. Field photos MP4037 and MP4255 show the appearance of the outcrops in this area (Figs. 14 and 15).

Figure 12. Field photo MP4148 showing water tank cut exposures at the north end of the cut (see Fig. 10). Weathered sandstone and shale (arrow "**sh**") seen at the top of this photo. Deeper in the cut are gray unweathered sandstone (~ 3 to 8 ft thick) with thin (<0.5 ft), lenticular shale interbeds. Well developed joints (arrow "**j**") terminate at the ~3 ft thick shale near the top of the cut.

Figure 13. Field photo MP4143. View to north showing area seen in Figure 12. This view shows prominent joints (arrows "**j**") in the thick unweathered Chatsworth sandstone terminating at the base of the 3 ft shale (arrow "**sh**").

Figure 14. Field photo MP4037 showing medium to thick bedded Chatsworth Fm. sandstone south of the Burro Flats Fault. The view is N60W. The sandstone here has a high density of joints (≥ 4.0/100) but with joints generally confined to individual beds. Figure 11 shows the location and view direction of this photo.

Figure 15. Field photo MP4255. View is to the SSE and looking nearly on edge of the west dipping Chatsworth sandstone across the gully. The trace of bedding, marked by the dashed lined, is obscured by the close-spaced joints in the sandstone. Such jointing is typical of the sandstone south of the western half of the Burro Flats Fault. See Figure 9 for the location of this photo.

Figure 16. Google Earth™ image location 16 (see Fig. 5 for location). Image shows close-spaced joints in Chatsworth sandstone in the area around the SSFL office. Both NW and NE trending joints are evident in this Google Earth image. In detail there can be complexites in joint patterns as pointed out by the arrows at "**a**" where joints fan from an ~N45W trend to a N15W trend. Also there is an indication of inverse variation of joint density with bed thickness. The thicker bed arrow "**b**" has a joint density of ~2.5/100 ft while the joint densities at the thinner beds at arrows "**a**" and "**c**" have joint densities of ~4.5/100 ft.

Figure 17. View of well-exposed surfaces of jointed Chatsworth sandstone beds. The center of this area is ~1 km N30W from the center of the Figure 8 area. In the northwestern part of this area a NW trending joint set is dominant with a joint density of ~2.3/100 ft while a secondary NE trending set consist of a few very prominent but wide-spaced joints (minor faults?) with a density of ~0.2/100 ft. In the central to east-central part of this area this is a curvilinear joint set with trends changing from ~N20W in the north to ~N45E in the south. A second joint set in this central area trends perpendicular to the curvilinear set. Joint density in this area is very high at ~4.0/100 ft.

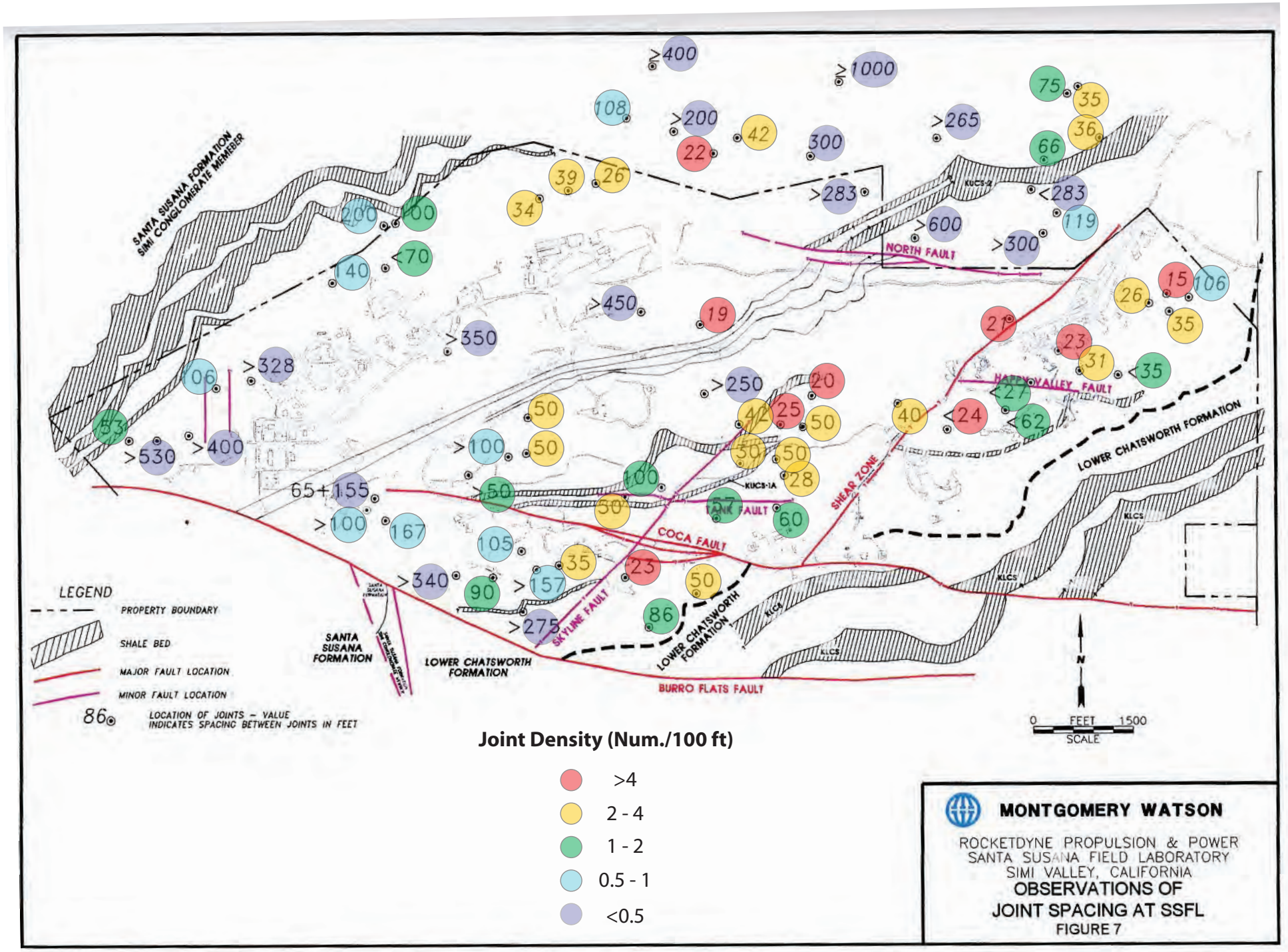

Figure 18. Joint Spacing/Density in Upper Chatsworth Fm. North of the Burro Flats Fault.

Figure 19. Google Earth image location 2 (see Fig. 5 for location). This image shows widely-spaced joints in Chatsworth sandstone. The dominant joint set here strikes northward, but a few ENE striking joints are visible in the thick sandstone bed in the center of this Google Earth image. In this 1600 ft wide sandstone channel only 2 throughgoing joints and one shorter joint are visible indicating a joint density of <0.2/100 ft.

Figure 20. Google Earth™ image location 20 (see Fig. 5 for location). This image shows the variable joint density in thick bedded Chatsworth sandstone in this area. The NW dipping sandstone in the center of this area ("**a**" arrows) is largely unjointed, though two minor, north striking faults cut this sandstone in the east central part of the area ("**b**" arrows). Above (NW of) the unjointed sandstone are two thick sandstone layers ("**c**" arrow) with a moderate joint density (~1.0/100 ft).

Figure 21. Google Earth™ image location #4 (see Fig. 5 for location). This image shows joints in thick bedded Chatsworth sandstone with low to moderate density (<=2.5/100 ft). Joints along individual traverses shown by circled numbers. The Burro Flats Fault (BFF) trends NW through the SW corner of this area. The COCA Fault trends WNW through the east-central part of this area with beds striking NE south of the western termination of the COCA Fault while striking ENE north of this termination.

Figure 22. Field photo MP4103. View SSW showing a set of close-spaced bedding normal joints in an amalgamated Chatsworth sandstone. This locality is just north of the Burro Flats Fault as shown on Figure 21. This outcrop is ~20 ft high. Arrow “b” points to bedding and arrow “j” points to one of the joints. See Figure 23 for an enlargement of the area to the left of arrow b.

Figure 23. Field photo MP4103 detail. Area to the left of arrow “b” in **Figure 22.** Field photo MP4103. Note the short length of many of the joints in this outcrop.

Figure 24. View northward showing thick sandstone/amalgamated sandstone beds (skyline ridge) in the Chatsworth Fm. north of the Burro Flats Fault. Note the wider spacing of joints in the thicker sandstone beds. The ridge in the middle ground is underlain by poorly exposed Chatsworth Fm. south of the Burro Flats Fault. The road in the foreground is in the bottom of Bell Canyon.

Figure 25. Field Photo 6/Oct/06-26. This photo shows a thin-bedded sandstone and shale unit in the Chatsworth Fm. Note the much higher density of joints in the sandstone (light colored layers). Less than 10% of the joints extend across more than one sandstone/ shale couplet and many of the irregular fractures in the shale are likely shrink-swell fractures formed during the recent surface weathering of these rocks.

Figure 26. Google Earth™ image location 26 (see Fig. 5 for location). This image shows the contrast in Chatsworth sandstone exposures across the Burro Flats Fault (BFF). Thick-bedded sandstone with low to moderate joint densities is well-exposed north of the fault. In contrast only a few patchy outcrops of sandstone are present south of the fault. Field work in the area south of the fault indicates that the Chatsworth Fm. here is mainly sandstone, but with beds possibly thinner, on average, than those on the north side of the fault. The sparsity of exposures south of the fault may reflect a higher joint density in this area. Arrow on the right side shows the direction of view of field photograph MP4048 (see Fig. 27).

Figure 27. View N80W (field photo MP4048). This photo shows sparsely jointed, thick bedded Chatsworth sandstone in the NE part of Google Earth™ image 26 (see Fig. 26 for location). Dashed line marks the approximate location of the Burro Flats Fault (BFF).